Pharmaceutical Research, Volume 23, No. 2, February 2006 (© 2006)
DOI: 10.1007/s11095-005-9259-4

Research Paper

Investigation of Wetting Behavior of Nonaqueous Ethylcellulose Gel Matrices Using Dynamic Contact Angle

L. W. Chan,[1] K. T. Chow,[1] and P. W. S. Heng[1,2]

Received July 4, 2005; accepted October 25, 2005

Purpose. This study reports the development of a method based on dynamic contact angle to investigate the wetting behavior of non-aqueous ethylcellulose (EC) gel matrices intended for topical drug delivery.
Methods. Non-aqueous gel matrices were prepared from the three fine particle grades of EC and propylene glycol dicaprylate/dicaprate. Dynamic contact angle measurements of sessile drops of water and isopropylmyristate (IPM) on EC gel matrices were performed using a dynamic contact angle analyzer equipped with axisymmetric drop shape analysis of the sessile drop images. Gel density was determined by weighing known volumes of gel samples.
Results. The EC gel matrices were wetted by both water and IPM, with much higher wettability by the latter. Increased EC concentration and polymeric chain length decreased the extent and rate of wetting. Linear correlation was observed between wetting parameters and rheological as well as mechanical properties of EC gel matrices.
Conclusions. The EC gel matrices exhibited both hydrophilic and lipophilic properties, with predominance of the latter. The extent and rate of wetting was governed by a balance of chemical and physical characteristics of the gel. EC gel matrices showed desirable wetting behavior in their function as a moisture-barrier, bioadhesive and vehicle for topical drug delivery.

KEY WORDS: Ethylcellulose; wetting; contact angle; rheology; surface configuration.

INTRODUCTION

Nonaqueous ethylcellulose (EC) gel was recently reported to be a useful topical drug delivery system because of its ability to form a structured gel network, which demonstrated satisfactory rheological and mechanical properties (1). The nonaqueous EC gel possessed advantages of lower gelling temperature, as well as superior properties as a vehicle for moisture-sensitive drug.

Apart from its rheological and mechanical properties, other pharmaceutically relevant properties of nonaqueous EC gel, such as wetting behavior, have not been reported. Wettability was shown to be an important predictor of compatibility and bioadhesion to skin and soft tissue substrates (2–5). Wettability was also cited as a prerequisite for drug release from hydrophobic tablet matrices, films, and coated beads (6–10). The significant predictive role of wettability in the aforementioned processes underlines the necessity of gaining a deeper understanding of the wetting behavior of EC gel matrices to correlate their applicability as a topical drug delivery system.

Static contact angles of water and other liquids have been widely used to characterize wetting properties (11), surface energies (12–14), as well as surface configurations of polymeric films and gels (15–17). Experiments involving contact angle measurement on pharmaceutical dosage forms were commonly carried out on samples in the form of casted films, dried coatings of gel on glass surfaces, or completely solidified blocks of gel. Pretreatment of gel samples ensures well-defined and flat solid surfaces with uniform thickness, which will possibly lead to more reproducible measurements. However, it may modify the sample surfaces that will almost inevitably alter the gel surface properties (10). Besides, the pretreated gel samples do not reflect the final usable form of the formulations. On account of these shortfalls, the use of the original gel matrices for contact angle measurement will certainly offer a more accurate and physiologically relevant representation of the gel wetting behavior. Although contact angle measurements have been widely reported for EC films and other cellulose ether films for coating applications (14,18), there has been no report of such measurement of EC gel matrices intended for topical application.

Water uptake ability of gel formulations is also used to indicate the degree of bioadhesion. This property is commonly determined by hydration study that involves immersion of the entire gel sample into an aqueous medium (19). However, topical gels are applied on relatively "dry" substrates, for instance, skin or buccal mucosa, and such applications by no means entail such an enormous amount of fluid medium as employed in hydration studies. Hence, a more appropriate method is necessary for the investigation of water uptake ability of topical gels. The dynamic contact angle measurement of

[1] Department of Pharmacy, Faculty of Science, National University of Singapore, 18 Science Drive 4, Singapore 117543, Singapore.
[2] To whom the correspondence should be addressed. (e-mail: phapaulh@nus.edu.sg)

small sessile water drops on topical gel matrices is a more appropriate method as the small drop size ensures the absence of drop deformation due to the influence of gravity, hence giving accurate contact angle values by axisymmetric drop shape analysis technique (20). The slight deformation of a large drop could also be easily detected using this technique. In addition, the small amount of liquid involved in the measurement mimics more closely the *in-use* conditions of the topical gel.

In view of the profound effect of wettability on product performance and the absence of pertinent wettability data on topical gel formulations, this study investigated the wetting behavior of nonaqueous EC gel matrices using dynamic contact angle. This study attempted to develop a method based on the dynamic contact angle of sessile liquid drops on nonaqueous EC gel matrices to characterize the wetting behavior of gels for topical application. Besides the well-known influence of polymer surface configuration, roughness, and chemical heterogeneity on the observed dynamic contact angles, it was hypothesized that rheological and mechanical properties of nonaqueous EC gel matrices also played a role in the gel wetting behavior when significant liquid absorption into gel matrices occurred.

MATERIALS AND METHODS

Materials

EC polymers of increasing chain length with ethoxyl content of 48.0–49.5%: Ethocel Std 7 FP Premium (EC7), Ethocel Std 10 FP Premium (EC10) and Ethocel Std 100 FP Premium (EC100), and propylene glycol dicaprylate/dicaprate (Miglyol 840) were gifts from Dow Chemical (Midland, MI, USA) and Sasol (Hamburg, Germany), respectively. Isopropylmyristate (IPM) was obtained from Sigma (St. Louis, MO, USA). Water used was of Milli-Q quality (Millipore, Billerica, MA, USA). Sigma Plot version 8.02 software for dynamic contact angle data analysis and curve-fitting was obtained from Systat Software (Point Richmond, CA, USA).

Determination of Polymer Molecular Weight

Molecular weights, M_w and M_n (g mol^{-1}), and polydispersity, M_w/M_n of EC7, EC10, and EC100 were obtained by gel permeation chromatography using Styragel column and reflective index detector (Models 2690, 2410, Waters, Milford, MA, USA) at 40°C. Tetrahydrofuran was the mobile phase and polystyrene standards were used. The results expressed as means from duplicated determinations are as follows: EC7, M_w = 54,068, M_n = 16,469, M_w/M_n = 3.3; EC10, M_w = 69,855, M_n = 27,533, M_w/M_n = 2.5; EC100, M_w = 130,273, M_n = 74,740, and M_w/M_n = 1.7.

Sample Preparations

EC was dissolved in the nonaqueous solvent (Miglyol 840) with continuous stirring at 60°C to form gels. Six formulations of different concentrations were prepared from each grade of EC, i.e., 11–16% w/w for EC7 and EC10, and 7–12% w/w for EC100. Gels were maintained at 22 ± 0.5°C for 24 h to ensure complete swelling prior to any testing.

Dynamic Contact Angle Measurements

Approximately 0.3 g of gel was carefully filled into a sample holder to avoid disruption of the gel structure. Excess gel was removed from the rim of the sample holder by using a spatula with sharp edges to produce a flat gel surface for dynamic contact angle measurement. The contact angles at the three-phase contact line, standing volumes, and base areas of sessile drops of water (θ_w, V_w, and A_w, respectively) and IPM (θ_i, V_i, and A_i, respectively) on the gel surface were measured using the FTÅ200 contact angle analyzer (First Ten Ångstroms, Portsmouth, VA, USA) equipped with a CCD camera (Sanyo, San Diego, CA, USA). The sessile drop was dispensed by a syringe pump through a 27-gauge, flat tip needle onto a flat surface of the gel. The volumes of each drop of water and IPM were approximately 8 and 3 μL, respectively. The change of contact angle was measured over time periods ranging from 1.5 to 4 min, and the captured images of the sessile drop were analyzed by the axisymmetric drop shape analysis technique using the FTÅ32 V2.0 Software. All measurements were performed at 22 ± 0.5°C in a humidity-controlled environment. The mean values of 6–10 sessile drops for each test liquid were reported. Dynamic contact angle measurements of sessile IPM drops were repeated on human skin to assess skin compatibility of IPM. Clean, untreated dorsal skin surfaces of the hands of six female and two male adult human volunteers aged between 25 and 31 years were used and the average value of at least three sessile drops of IPM in each volunteer was reported. The area of the skin was cleaned by gentle wiping using tissue paper wetted with distilled water. To ensure that the effect of sessile water drop evaporation was negligible, dynamic contact angle measurement was also carried out for sessile water drop on an impermeable solid surface, and the rate of change of standing volume was obtained.

Determination of IPM Surface Tension

The surface tension of IPM was measured at 22 ± 2°C using the Wilhelmy plate method (Rosano, Roller Smith; Biolar Corp., North Grafton, MA, USA). A correction factor due to the thermal expansion of plate was included in the calculation of surface tension.

Determination of Gel Density

A shallow acrylate container (depth: 3 mm, diameter: 50 mm) with a cover was employed for gel density measurement. Freshly prepared EC gel was filled to slight excess and maintained for 24 h. The cover was carefully put in place and excess gel was removed. The weight of gel was determined at 22 ± 0.5°C. The volume of each container was determined by measuring the weight of water under the same experimental conditions. The average gel density values from at least three samples were reported. Gel density was calculated as follows:

$$\text{Gel Density} = (\text{Weight of Gel}/\text{Weight of Water}) \times 0.998\,\text{g ml}^{a}$$

[a]Water density at 22°C, Ref. (21).

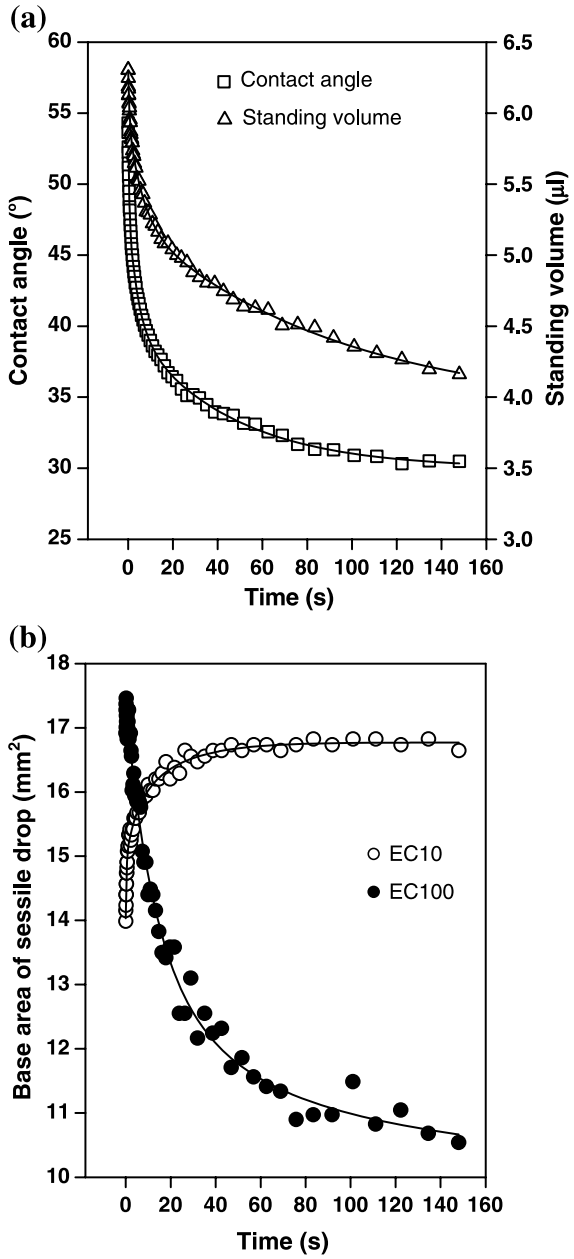

Fig. 1. (a) Contact angle and standing volume vs. time profiles of sessile water drop on 12% w/w EC10 gel matrices. (b) Base area vs. time profiles of sessile water drop on 12% w/w EC10 and 7% w/w EC100 gel matrices.

Statistical Analysis

All results were statistically evaluated using one-way ANOVA. Post-hoc statistical analyses of the means of individual groups were performed using Tukey's test. For all analyses, $p < 0.05$ denoted significance.

RESULTS

The surfaces of EC gel matrices used for the dynamic contact angle measurement were observed to be distinct and flat to give a well-defined baseline for drop shape analysis. The wetting of EC gels by water and IPM was interpreted in terms of the extent and rate of wetting. The wetting of a sessile liquid drop on a surface is governed by the balance of interfacial, gravitational, viscous, and inertial forces. For small liquid drops like those employed in this study, wetting phenomenon was only governed by interfacial forces where other forces acting on the liquid drop were negligible for reasons explained elsewhere (22,23). On this basis, a hemispherical section could be assumed for liquid drop on the gel surface.

Wetting of EC Gels by Sessile Water Drops

Plots of θ_w vs. time and the corresponding V_w of all EC gels followed an exponential decay toward an equilibrium value. A_w was observed to rise exponentially with time toward a plateau (Fig. 1). However, it should be noted that the reported contact angles were possibly in the metastable equilibrium state instead of the true stable equilibrium state, because the latter could only be obtained on an ideal solid surface (24). The θ_w, V_w, and A_w profiles were best fitted to an exponential model, $f(x) = y_0 + ae^{-bx} + ce^{-dx} + ge^{-hx}$, where y_0, a, b, c, d, e, g, and h are constants. This model was used to compute the equilibrium θ_w, V_w, and A_w values at t = 300 s, which represented the extent of EC gel wetting by water. This time point was chosen for the purpose of standardization across all the different EC gel formulations with the assumption that 300 s was sufficiently long for the sessile water drop contact angle to reach equilibrium. The same model was used to obtain $t_{50\%}$ values, defined as the time taken to for θ_w, V_w, and A_w to decrease by 50% from their initial values. This parameter was useful in describing the rate of EC gel wetting. Effect of water drop evaporation was insignificant as the rate of decrease in sessile water drop standing volume on an impermeable solid surface was only 0.002 µL s^{-1}, which was negligible. The reliability of the proposed exponential model to extrapolate θ_w, V_w, and A_w accurately to t = 300 s had been validated by axisymmetric drop shape analysis of images of the same samples taken as snapshots (single images) after 300 s. The mean measured values of θ_w, V_w, and A_w of sessile water drops on EC gels obtained over a range of time after 300 s are presented in Table I. The low percentage deviation (≤8.6%) of the predicted (extrapolated) values from the measured values of θ_w, V_w, and A_w for the samples verified the accuracy of the equilibrium values obtained from extrapolation to t = 300 s.

The initial (t = 0) and equilibrium (t = 300 s) θ_w, V_w, and A_w, as well as the ratio and % change of these parameters, were employed to describe the extent of EC gel wetting by water (Table II). The initial θ_w ($\theta_{w/0}$), equilibrium θ_w ($\theta_{w/e}$), and $\theta_{w/e}/\theta_{w/0}$ ratio exhibited an upward trend with an increase in polymer concentration for all the EC gels, whereas the % change of θ_w ($\Delta\theta_w$) exhibited the opposite trend (Table II). The decrease in θ_w over time was a result of absorption and/or spreading of the sessile water drop upon contact with the gel matrices. Absorption was manifested by a reduction of V_w while spreading by an increase in A_w over time.

The initial V_w ($V_{w/0}$), equilibrium V_w ($V_{w/e}$), $V_{w/e}/V_{w/0}$ ratio, and % change of V_w (ΔV_w) demonstrated similar concentration-dependent trend as the corresponding parameters for θ_w. The decrease in ΔV_w from 35 to 20%, 39 to 17%, and 76 to 8% when EC concentration increased for EC7,

Table I. Comparison Between the Predicted and Measured Equilibrium Contact Angle, Base Area, and Standing Volume of Sessile Water Drops on EC Gels

EC (% w/w)	Contact angle (°)			Base area (mm^2)			Standing volume (μL)			Time range[b] (s)	N[c]
	Predicted[a]	Measured	% Deviation	Predicted[a]	Measured	% Deviation	Predicted[a]	Measured	% Deviation		
EC7											
11	32.5	31.6 ± 1.6	2.8	19.8	19.4 ± 0.7	2.1	4.7	4.9 ± 0.4	4.1	586–817	9
16	43.2	41.9 ± 0.9	3.1	18.2	18.6 ± 0.4	2.2	6.3	6.3 ± 0.2	0.0	575–718	9
EC10											
11	29.0	27.8 ± 1.4	4.3	18.1	17.2 ± 1.0	5.2	3.8	3.5 ± 0.3	8.6	390–576	9
16	43.5	43.2 ± 0.7	0.7	18.0	18.0 ± 0.3	0.0	6.3	6.3 ± 0.2	0.0	318–318	9
EC100											
8	35.8	36.0 ± 1.4	0.6	17.7	17.9 ± 1.8	1.1	4.8	5.0 ± 0.6	4.0	377–471	9
12	48.3	46.1 ± 0.9	4.8	17.9	18.8 ± 0.6	4.8	7.5	7.2 ± 0.3	4.2	298–390	10

[a] Equilibrium contact angle, base area, and standing volume values are adapted from Table II.
[b] The range of time where snapshots of sessile water drop were taken.
[c] Sample size.

EC10 and EC100, respectively, indicated that water was being absorbed into the matrices of all the EC gels such that lower degree of water absorption was observed for gels with higher EC concentration.

The extent of spreading of the sessile water drop was described by initial A_w ($A_{w/0}$), equilibrium A_w ($A_{w/e}$), and $A_{w/e}/A_{w/0}$ ratio. The A_w profile of 7% w/w EC100 followed an exponential decay (Fig. 1) instead of the typical profiles of exponential rise to plateau as shown by other concentrations and grades of EC gels. Spreading was hindered as a result of prominent degree of water absorption into this gel matrix, hence water spreading was not relevant for this particular formulation. Unlike the other parameters, $A_{w/0}$, $A_{w/e}$, and $A_{w/e}/A_{w/0}$ ratio did not show any significant trend with EC concentration and polymeric chain length. $A_{w/e}/A_{w/0}$ ratio was about 1.2 for all the EC gels tested except for 7% w/w EC100, which showed an $A_{w/e}/A_{w/0}$ ratio of 0.7. An $A_{w/e}/A_{w/0}$ ratio of greater than 1 indicated spreading and ratio of less than 1 indicated absorption of sessile water drop.

$\theta_{w/0}$, $\theta_{w/e}$, $\theta_{w/e}/\theta_{w/0}$ ratio, $\Delta\theta_w$, and the corresponding parameters for V_w exhibited linear relationship with EC concentration for 11–16% w/w EC7 and EC10, and 8–12% w/w EC100 (Fig. 2). Most of these parameters for 7% w/w EC100 were found to be exceptionally low and $A_{w/e}$ was less than $A_{w/0}$, indicating water absorption without spreading. The change in θ_w observed in the rest of the EC gel samples could be accounted for by both spreading and absorption. The relatively low θ_w and V_w values for 7% w/w EC100 were more apparent at equilibrium as compared to initial state because time was needed for significant absorption into the gel matrices. $\theta_{w/e}/\theta_{w/0}$, $V_{w/e}/V_{w/0}$, and $A_{w/e}/A_{w/0}$ ratio were regarded as relatively more accurate parameters to indicate extent of wetting as possible errors caused by small change in drop volume could be avoided.

Comparing the influence of different polymeric chain lengths, EC100 was found to have much higher $\theta_{w/e}/\theta_{w/0}$ and $V_{w/e}/V_{w/0}$ ratios (Fig. 2), as well as lower $\Delta\theta_w$ and ΔV_w than EC7 and EC10 (Table II). These parameters were not significantly different ($p > 0.05$, one-way ANOVA) between EC7 and EC10, probably because the difference in their molecular weights was relatively small. The absolute values of θ_w and V_w of EC100 were also much higher. The concentration dependence of $V_{w/0}$ and $V_{w/e}$ increased in the order of EC7 < EC10 < EC100, as shown by the slope values of 0.1211 and 0.3549, respectively, for EC7; 0.3251 and 0.5387, respectively, for EC10; and 0.4122 and 0.6913, respectively, for EC100. This implied that reduction in water absorption capacity was more sensitive to EC concentration as polymeric chain length increased, hence reflecting the prominent role of polymeric chain length in the wetting property of EC gels. Similar trends were demonstrated by the slopes of $\theta_{w/0}$ and $\theta_{w/e}$ vs. concentration profiles with the exception of $\theta_{w/0}$ profiles between EC7 and EC10, which did not exhibit statistically significant difference in their slopes. Because A_w did not show any significant trend with EC concentration or polymeric chain length, the concentration dependence of $\theta_{w/0}$ and $\theta_{w/e}$ could be primarily attributed to water absorption.

The rate of EC gel wetting by water was determined by kinetic modeling of the rate of change of θ_w, V_w, and A_w from 2 to 12 s. The change in these values markedly slowed

Table II. EC Gel Wetting Parameters by Water as Represented by Sessile Water Drop Contact Angle (θ_w), Standing Volume (V_w), Base Area (A_w), and Rate Constant for Contact Angle, $K_{\theta w}$

EC (% w/w)	Initial θ_w (°)	Equilibrium θ_w (°)	θ_w change (%)	$\theta_{w/e}/\theta_{w/0}$ ratio	Initial V_w (μL)	Equilibrium V_w (μL)	V_w change (%)	$V_{w/e}/V_{w/0}$ ratio	Initial A_w (mm^2)	Equilibrium A_w (mm^2)	A_w change (%)	$A_{w/e}/A_{w/0}$ ratio	$K_{\theta w}$ (s^{-1})
EC7													
11	56.1 ± 1.4	32.5 ± 1.9	42.1	0.58 ± 0.02	7.3 ± 0.2	4.7 ± 0.4	35.3	0.64 ± 0.04	16.1 ± 0.3	19.8 ± 0.7	22.9	1.23 ± 0.04	0.043 ± 0.003
12	55.5 ± 0.9	32.2 ± 1.9	42.0	0.58 ± 0.03	7.3 ± 0.3	4.8 ± 0.4	33.6	0.67 ± 0.06	16.0 ± 0.6	19.8 ± 1.0	23.4	1.23 ± 0.05	0.042 ± 0.007
13	57.2 ± 1.6	35.3 ± 1.9	38.2	0.62 ± 0.04	7.2 ± 0.5	5.0 ± 0.5	30.7	0.72 ± 0.09	15.2 ± 0.7	18.6 ± 1.7	22.6	1.22 ± 0.08	0.040 ± 0.004
14	60.6 ± 1.1	37.9 ± 1.5	37.4	0.63 ± 0.03	7.5 ± 0.3	5.8 ± 0.5	22.2	0.78 ± 0.05	15.0 ± 0.4	19.2 ± 1.1	27.8	1.28 ± 0.07	0.039 ± 0.003
15	60.5 ± 1.1	41.2 ± 1.7	31.9	0.68 ± 0.03	7.7 ± 0.3	6.1 ± 0.3	20.6	0.79 ± 0.04	15.4 ± 0.4	18.6 ± 0.7	20.9	1.21 ± 0.03	0.031 ± 0.003
16	61.4 ± 1.0	43.2 ± 0.9	29.7	0.70 ± 0.02	7.8 ± 0.2	6.3 ± 0.4	19.9	0.80 ± 0.04	15.3 ± 0.3	18.2 ± 0.5	19.0	1.19 ± 0.02	0.029 ± 0.003
EC10													
11	52.5 ± 0.6	29.0 ± 1.9	44.8	0.55 ± 0.03	6.3 ± 0.3	3.8 ± 0.4	39.3	0.60 ± 0.04	15.3 ± 0.5	18.1 ± 1.2	18.0	1.18 ± 0.06	0.057 ± 0.006
12	55.4 ± 1.9	33.0 ± 2.4	40.5	0.60 ± 0.04	6.4 ± 0.3	4.1 ± 0.5	35.1	0.65 ± 0.06	14.8 ± 0.5	17.7 ± 0.7	19.5	1.20 ± 0.06	0.050 ± 0.004
13	57.3 ± 1.3	36.0 ± 1.6	37.2	0.63 ± 0.03	6.7 ± 0.6	5.0 ± 0.5	25.9	0.74 ± 0.03	14.8 ± 0.8	18.0 ± 1.3	22.0	1.22 ± 0.04	0.047 ± 0.004
14	58.7 ± 1.2	38.3 ± 1.0	34.6	0.65 ± 0.02	7.5 ± 0.3	5.7 ± 0.4	24.1	0.76 ± 0.04	15.6 ± 0.5	19.0 ± 0.8	21.9	1.22 ± 0.05	0.032 ± 0.004
15	59.0 ± 1.0	42.7 ± 0.9	27.7	0.72 ± 0.01	7.8 ± 0.3	6.1 ± 0.3	21.7	0.78 ± 0.01	15.6 ± 0.3	18.4 ± 0.5	17.6	1.18 ± 0.03	0.026 ± 0.002
16	59.8 ± 1.0	43.4 ± 0.7	27.3	0.73 ± 0.01	7.6 ± 0.3	6.3 ± 0.2	17.3	0.83 ± 0.02	15.4 ± 0.6	18.0 ± 0.4	16.6	1.17 ± 0.03	0.025 ± 0.002
EC100													
7	44.4 ± 2.4	19.3 ± 2.6	56.5	0.43 ± 0.04	5.6 ± 0.5	1.4 ± 0.5	75.5	0.24 ± 0.07	17.0 ± 0.7	11.5 ± 2.2	−31.9	0.68 ± 0.12	0.069 ± 0.011
8	52.9 ± 1.4	35.8 ± 2.5	32.3	0.68 ± 0.04	6.4 ± 0.5	4.8 ± 0.5	24.5	0.74 ± 0.07	15.4 ± 0.7	17.7 ± 1.5	15.2	1.15 ± 0.07	0.041 ± 0.006
9	55.7 ± 1.5	39.3 ± 1.3	29.4	0.71 ± 0.03	6.8 ± 0.5	5.4 ± 0.6	20.3	0.79 ± 0.08	15.2 ± 0.6	18.1 ± 1.3	18.7	1.19 ± 0.05	0.040 ± 0.003
10	58.1 ± 1.8	43.3 ± 1.7	25.4	0.75 ± 0.01	6.8 ± 0.7	6.1 ± 0.6	10.6	0.85 ± 0.04	14.7 ± 0.6	17.4 ± 1.2	18.8	1.19 ± 0.04	0.042 ± 0.004
11	60.2 ± 1.9	46.9 ± 1.5	22.1	0.78 ± 0.02	7.4 ± 0.3	6.8 ± 0.5	8.8	0.91 ± 0.04	15.0 ± 0.7	18.0 ± 0.7	20.0	1.20 ± 0.04	0.049 ± 0.004
12	61.4 ± 1.3	48.3 ± 1.1	21.3	0.78 ± 0.02	8.1 ± 0.5	7.5 ± 0.5	8.2	0.92 ± 0.03	15.7 ± 0.7	17.9 ± 1.7	14.0	1.21 ± 0.03	0.053 ± 0.006

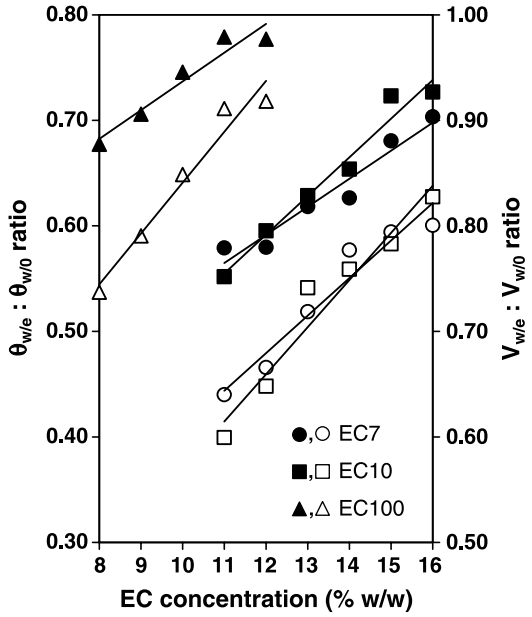

Fig. 2. Linear relationship between equilibrium/initial contact angle ratio ($\theta_{w/e}/\theta_{w/0}$) and equilibrium/initial standing volume ratio ($V_{w/e}/V_{w/0}$) of sessile water drop and EC concentrations with correlation coefficients, $r = 0.9696$ (●), $r = 0.9691$(○), $r = 0.9846$ (■), $r = 0.9716$ (□), $r = 0.9655$ (▲), and $r = 0.9797$ (△). Closed symbols represent $\theta_{w/e}/\theta_{w/0}$ and open symbols represent $V_{w/e}/V_{w/0}$.

down after 10 s. The decline in θ_w with time followed first-order kinetics (25) as linear plots of $\ln(\theta_w - \theta_{w/e})$ vs. time were obtained for all the EC gels [correlation coefficient (r) = 0.9359–0.9951] with rate constants of $K_{\theta w}$ (Fig. 3). Both V_w and A_w fitted into the same kinetic model. Despite the acceptable r values, it should be noted that direct kinetic modeling as shown above might not be adequate to study the wetting kinetics of EC gels because it involved both water

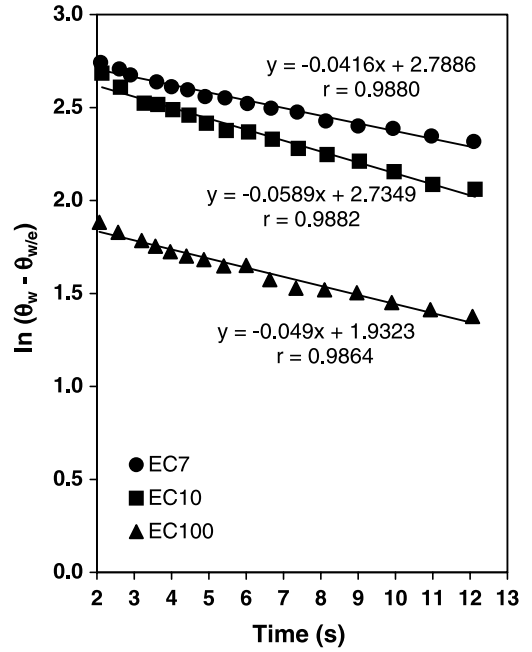

Fig. 3. Decline in contact angle, θ_w, of sessile water drop with time according to first-order kinetics. First-order rate constants are given by slopes of the linear regressions.

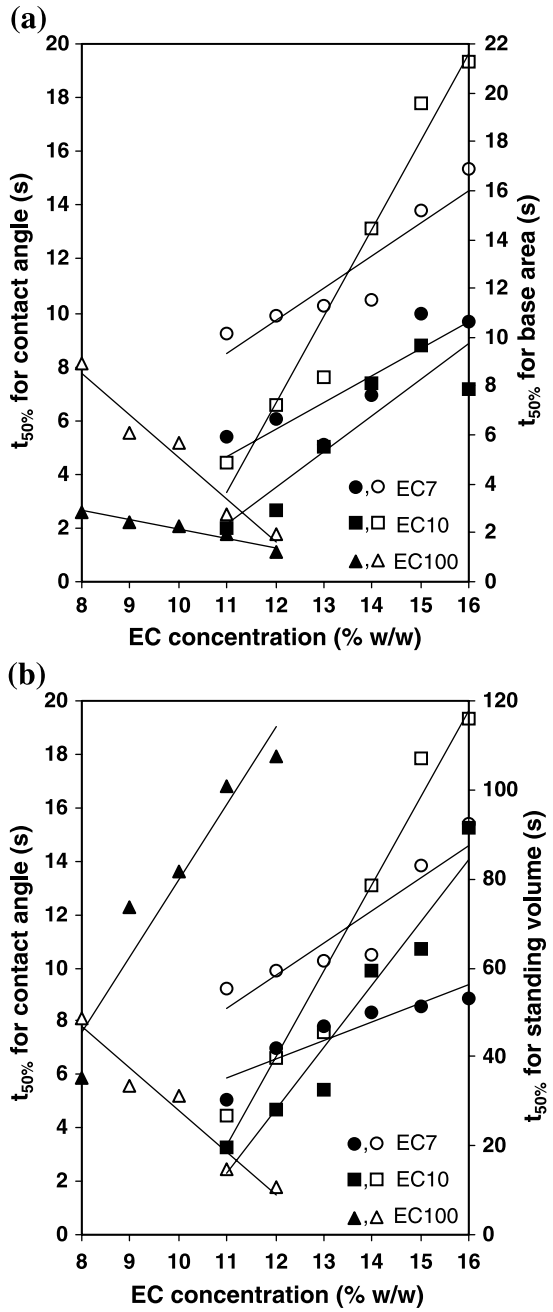

Fig. 4. Change in (a) contact angle and standing volume $t_{50\%}$ and (b) contact angle and base area $t_{50\%}$ of sessile water drop with EC concentration. Correlation coefficients for contact angle, $r = 0.9226$ (○), $r = 0.9777$ (□), $r = 0.9744$ (△); base area, $r = 0.8742$ (●), $r = 0.9082$ (■), $r = 0.9697$ (▲); and standing volume, $r = 0.9220$ (●), $r = 0.9697$ (■), $r = 0.9550$ (▲). Closed symbols represent base area or standing volume and open symbols represent contact angle.

spreading and absorption at the same time. However, kinetic constants derived from such simple modeling could still provide useful comparison among the different gel formulations. $K_{\theta w}$ was generally low, with values ranging from 0.025 to 0.069 s^{-1}. There was a slight decrease in rate of gel wetting by water at higher concentration ranges of both EC7 and EC10 (Table II). It was interesting to note that $K_{\theta w}$ values of 11 and 12% w/w EC100 were significantly higher

Table III. The Free Energy Change Involved in Adhesional, Immersional, and Spreading Wetting of EC Gels by Water Sessile Drop

EC (% w/w)	Work of adhesion (mJ m^{-2})	Adhesion tension (mJ m^{-2})	Spreading coefficient (mJ m^{-2})
EC7			
11	134.2 ± 1.3	61.4 ± 1.3	−11.4 ± 1.3
12	134.4 ± 1.3	61.6 ± 1.3	−11.2 ± 1.3
13	132.2 ± 1.4	59.4 ± 1.4	−13.4 ± 1.4
14	130.2 ± 1.2	57.4 ± 1.2	−15.4 ± 1.2
15	127.6 ± 1.5	54.8 ± 1.5	−18.0 ± 1.5
16	125.9 ± 0.8	53.1 ± 0.8	−19.7 ± 0.8
EC10			
11	136.5 ± 1.2	63.7 ± 1.2	−9.3 ± 1.1
12	133.8 ± 1.7	61.0 ± 1.7	−12.4 ± 1.4
13	131.7 ± 1.1	58.9 ± 1.1	−13.9 ± 1.1
14	129.9 ± 0.8	57.1 ± 0.8	−15.7 ± 0.8
15	126.3 ± 0.8	53.5 ± 0.8	−19.3 ± 0.8
16	125.6 ± 0.7	52.8 ± 0.7	−20.0 ± 0.7
EC100			
7	141.5 ± 1.1	68.7 ± 1.1	−3.6 ± 0.6
8	131.8 ± 1.8	59.0 ± 1.8	−14.2 ± 1.6
9	129.2 ± 1.0	56.4 ± 1.0	−16.4 ± 1.0
10	125.7 ± 1.5	52.9 ± 1.5	−19.9 ± 1.5
11	122.5 ± 1.4	49.7 ± 1.4	−23.1 ± 1.4
12	121.8 ± 1.1	49.0 ± 1.1	−23.8 ± 1.1

Water surface tension of 72.8 mN m^{-1} was employed for calculation.

Table IV. EC Gel Wetting Parameters by IPM as Represented by Sessile IPM Drop Contact Angle (θ_i), Standing Volume (V_i), and Rate Constant for Contact Angle, $K_{\theta i}$

EC (% w/w)	Initial θ_i (°)	Initial V_i (μL)	$K_{\theta i}$ (s^{-1})
EC7			
11	17.3 ± 1.3	2.2 ± 0.3	0.32 ± 0.02
12	21.7 ± 1.9	2.2 ± 0.2	0.31 ± 0.03
13	23.1 ± 2.0	2.3 ± 0.3	0.32 ± 0.03
14	23.7 ± 1.8	2.4 ± 0.2	0.31 ± 0.03
15	25.2 ± 1.5	2.5 ± 0.2	0.33 ± 0.03
16	27.2 ± 1.1	2.6 ± 0.2	0.31 ± 0.03
EC10			
11	18.3 ± 1.6	2.5 ± 0.3	0.44 ± 0.07
12	20.6 ± 2.2	2.5 ± 0.3	0.35 ± 0.04
13	21.5 ± 1.8	2.6 ± 0.1	0.34 ± 0.03
14	21.0 ± 2.6	2.5 ± 0.1	0.33 ± 0.04
15	23.6 ± 1.7	2.8 ± 0.3	0.33 ± 0.03
16	26.5 ± 1.8	2.8 ± 0.2	0.33 ± 0.05
EC100			
7	15.8 ± 1.3	2.1 ± 0.3	0.90 ± 0.09
8	21.4 ± 2.0	2.4 ± 0.2	0.44 ± 0.08
9	23.2 ± 1.8	2.5 ± 0.1	0.39 ± 0.03
10	26.4 ± 1.7	2.7 ± 0.2	0.30 ± 0.04
11	29.2 ± 1.9	2.7 ± 0.1	0.28 ± 0.03
12	31.0 ± 2.1	2.8 ± 0.2	0.23 ± 0.02

than those of 8–10% w/w, which indicated more rapid wetting at higher EC100 concentration. EC100 gel at 7% w/w exhibited a particularly high $K_{\theta w}$ due to its absorption-dominated mechanism of wetting. The $t_{50\%}$ values derived from the plots of θ_w, V_w, and A_w vs. time were found to be less reproducible but they exhibited trends that could aid in interpretation of the rate constants. The trends of $K_{\theta w}$ vs. EC concentration were supported by the $t_{50\%}$ values of θ_w, which showed a concomitant concentration-dependent increase for EC7 and EC10, and concentration-dependent decrease for EC100 from 8% w/w onwards (Fig. 4). The main process responsible for the observed trend of $K_{\theta w}$ could be envisaged by examining the rate of water absorption and spreading. The $t_{50\%}$ values for V_w (Fig. 4) indicated a concentration-dependent decrease in rate of water absorption for all the EC gels. The $t_{50\%}$ values for A_w and θ_w showed similar trends, indicating that the rate of spreading played a major role in influencing $K_{\theta w}$. Therefore, the faster wetting of gels with higher EC100 concentration was primarily attributed to faster liquid spreading rather than faster liquid absorption. It should be noted that the rate of wetting only reflected how rapidly the sessile water drop attained equilibrium state. Higher rate of wetting might not necessarily indicate higher extent of wetting as shown by EC100 gels, where rate of wetting was higher in gels with higher EC100 concentration but the extent of wetting was still lower.

Classically, the wetting process is described by three different stages, that is, adhesional, immersional, and spreading wetting. The free energy change involved in the respective stages of wetting is represented by W_a (work of adhesion), A_t (adhesion tension), and S_c (spreading coefficient), which are defined as follows (26): $W_a = \gamma_{LV}(\cos\theta + 1)$, $A_t = \gamma_{LV}\cos\theta$, and $S_c = \gamma_{LV}(\cos\theta - 1)$, where γ_{LV} denotes the surface tension of the wetting liquid and θ denotes the contact angle. It should be noted that W_a, A_t, and S_c for EC gels at equilibrium (t = 300 s), as presented in Table III, might not necessarily be the true free energy values as the above-mentioned equations employed for calculation were derived from Young's equations for solid substrate with ideal smooth surface. However, these energy values could be employed as a relative gauge on the mechanism involved in EC gel

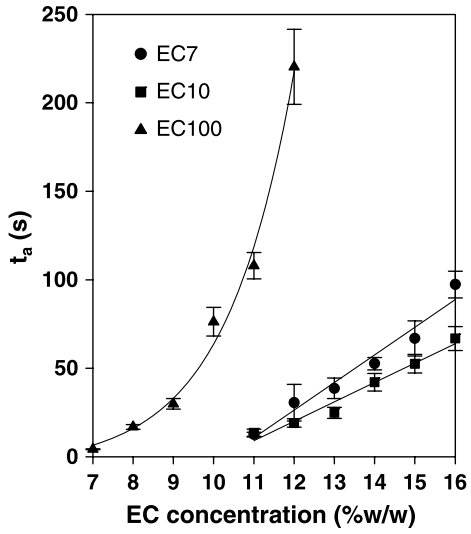

Fig. 5. Time for complete absorption of sessile IPM drops into EC gel matrices, t_a, as a function of EC concentration.

Table V. Comparison of the Extent and Rate of EC Gel Wetting by Water and IPM

	Ratio	
EC (% w/w)	$\theta_{w/0}\theta_{i/0}$	$K_{\theta i}/K_{\theta w}$
EC7		
11	3.2	7.4
12	2.6	7.2
13	2.5	8.0
14	2.6	8.0
15	2.4	10.5
16	2.3	10.9
EC10		
11	2.9	7.7
12	2.7	7.1
13	2.7	7.2
14	2.8	10.3
15	2.5	13.0
16	2.3	13.2
EC100		
7	2.8	13.1
8	2.5	10.8
9	2.4	9.7
10	2.2	7.2
11	2.1	5.7
12	2.0	4.4

Difference in extent and rate of wetting is expressed as ratio between the initial contact angle of water, $\theta_{w/0}$, and IPM, $\theta_{i/0}$, for the former, and ratio between the contact angle rate constant of IPM, $K_{\theta i}$, and water, $K_{\theta w}$, for the latter.

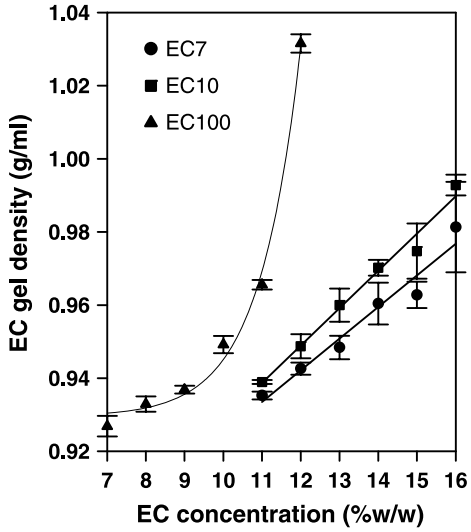

Fig. 6. Change of EC gel density as a function of EC concentration.

wetting as well as a means of comparison among the different EC gels studied for the same wetting liquid. Positive W_a and A_t (Table III) reflected spontaneous adhesional and immersional wetting of EC gels by water, whereas negative S_c indicated absence of complete water spreading. There was a significant decrease ($p < 0.05$, one-way ANOVA) in W_a, A_t, and S_c when EC concentration was increased in the EC gels. W_a, A_t, and S_c values were comparable for most concentrations of EC7 and EC10 gels, but were significantly lower in EC100 gels. Hence, the thermodynamic driving force for

Table VI. Rheological and Mechanical Parameters of EC Gels[a]

EC (% w/w)	Elastic modulus (Pa)	Apparent viscosity (mPa s)	Yield stress (Pa)	Hysteresis area (Pa s^{-1})	Hardness (mN)	Adhesiveness (N mm)
EC7						
11	47.1 ± 6.1	7,154 ± 768	36.2 ± 6.1	1,515 ± 217	263 ± 26	3.0 ± 0.2
12	69.6 ± 4.8	10,359 ± 354	52.5 ± 3.8	2,207 ± 211	414 ± 31	4.4 ± 0.4
13	88.9 ± 4.8	15,306 ± 601	77.5 ± 2.7	3,066 ± 124	1,395 ± 136	13.4 ± 0.7
14	121.7 ± 10.2	21,415 ± 373	103.3 ± 2.7	4,006 ± 171	1,993 ± 129	21.0 ± 1.5
15	152.2 ± 6.2	25,623 ± 373	107.1 ± 2.2	4,084 ± 49	2,402 ± 150	26.7 ± 2.6
16	178.7 ± 8.1	34,342 ± 642	137.8 ± 2.8	4,772 ± 166	3,277 ± 69	36.7 ± 2.5
EC10						
11	67.3 ± 8.9	12,225 ± 171	63.1 ± 8.1	2,263 ± 147	1,522 ± 73	13.4 ± 2.1
12	89.8 ± 12.8	16,017 ± 744	85.4 ± 4.9	3,064 ± 216	1,829 ± 154	16.8 ± 2.2
13	114.2 ± 11.5	19,833 ± 1,154	102.8 ± 5.8	3,727 ± 321	2,163 ± 211	20.8 ± 3.2
14	174.8 ± 8.9	28,525 ± 1,106	142.4 ± 1.9	4,660 ± 284	2,536 ± 164	27.8 ± 1.6
15	208.8 ± 26.2	41,466 ± 1,402	200.1 ± 11.4	5,838 ± 516	3,244 ± 114	37.9 ± 1.5
16	278.7 ± 19.1	60,616 ± 1,855	333.0 ± 18.4	7,093 ± 419	6,031 ± 436	61.9 ± 5.6
EC100						
7	24.2 ± 2.1	3,250 ± 235	12.8 ± 1.8	575 ± 86	383 ± 11	3.2 ± 0.5
8	160.0 ± 14.0	8,086 ± 361	41.6 ± 3.4	1,428 ± 91	674 ± 61	7.0 ± 0.2
9	212.3 ± 18.5	15,589 ± 660	85.2 ± 5.7	2,334 ± 175	1,298 ± 90	14.5 ± 0.7
10	343.2 ± 32.3	25,789 ± 509	143.4 ± 5.0	3,363 ± 151	2,314 ± 232	25.7 ± 3.4
11	664.4 ± 55.9	40,278 ± 790	222.3 ± 7.9	4,090 ± 377	3,778 ± 95	47.5 ± 3.4
12	937.6 ± 93.1	60,600 ± 2,607	365.2 ± 19.7	5,311 ± 493	5,098 ± 349	68.8 ± 5.2

[a] Data adopted from Ref. (1).

each type of wetting decreased with increase in EC concentration and polymeric chain length.

Wetting of EC gels by Sessile IPM Drops

Plots of θ_i, V_i, and A_i vs. time followed an exponential decay and were also found to be best fitted to the same exponential model as that for water. Instead of forming an equilibrium sessile drop on the EC gel surface, IPM was completely absorbed into the gel matrices. Therefore, the extent of EC gel wetting by IPM could only be evaluated by the $\theta_{i/0}$ and $V_{i/0}$, namely, θ_i and V_i at $t = 0$, respectively (Table IV). $\theta_{i/0}$, with coefficients of variation (CV) of less than 10% for most formulations, was relatively more consistent than $V_{i/0}$, which exhibited CV ranging from 4 to 20% with the latter occurring in gels at lower concentration range of EC. There was a fairly linear concentration-dependent trend for both $\theta_{i/0}$ ($r \geq 0.9385$) and $V_{i/0}$ ($r \geq 0.8780$) for the entire range of EC concentrations used in the study. For IPM, the $\theta_{i/0}$ and $V_{i/0}$ of 7% w/w EC100 were able to fit into the respective linear regressions as opposed to the observation made on water because the wetting of EC gel by IPM was dominated by the same mechanism for the entire concentration range of EC100, namely, absorption. For gel concentrations of 11 and 12% w/w, EC100 showed significantly higher $\theta_{i/0}$ than both EC7 and EC10. The base area for IPM sessile drops was rather erratic as observed from the high CV, probably due to the fast absorption of this liquid by EC gel. Therefore, base area was not employed to describe the extent of gel wetting by IPM as it was deemed to be unreliable.

The rate of EC gel wetting by IPM could be described by the rate constant, $K_{\theta i}$ (Table IV) and time taken for a complete IPM absorption, t_a. These two parameters basically described the rate of IPM absorption. Linear plots of $\ln\theta_i$ vs. time were obtained from 0.1 to 3 s (r = 0.8686–0.9917), indicating wetting of EC gels by IPM according to first-order kinetics. The initial rapid decline of θ_i was observed to slow down after approximately 3 s for all the EC gel formulations. No significant trend between $K_{\theta i}$ and EC concentration was observed for all the formulations of EC7 and EC10, except 11% w/w EC10. On the contrary, a significant decrease in $K_{\theta i}$ was exhibited with an increase in EC100 concentration. This showed that the rate of wetting of EC gels with longer polymeric chain was more sensitive to polymer concentration than those of shorter polymeric chains. Time taken for complete absorption of IPM ranged from 12.5 to 220.3 s. EC7 and EC10 showed a linear increase in t_a with increasing polymer concentration (Fig. 5). For EC100, the increase was exponential, where influence of EC concentration was much more prominent at concentration above 9% w/w.

The W_a and S_c values of IPM on EC gels was 58.1 and 0.0 mJ m^{-2}, respectively, indicating spontaneous adhesional and spreading wetting. Calculations of W_a and S_c were based on $\theta = 0°$ from the complete wetting of EC gels by IPM, and γ_{LV} = 29.0 mN m^{-1}, as determined from the Wilhelmy plate method. For $\theta \leq 0°$, A_t could not be determined from contact angle. It required alternative methods such as calorimetry to measure the heat of immersion (26), which was not performed in this study. Nevertheless, immersional wetting of EC gels was evident because A_t would be positive as long as $\theta < 90°$ (27).

Comparison was made for the wetting of EC gel by water and IPM. The initial contact angles of water sessile drop on EC gel matrices were 2- to 3-fold higher than those of IPM, indicating a higher extent of EC gel wetting by IPM. The rates of wetting by IPM were 4- to 13-fold higher than water in all the EC gels studied (Table V).

Wetting of Human Skin by Sessile IPM Drops

IPM was found to be readily absorbed into human skin with initial contact angle, $\theta_{i/h}$, ranging from 22.5 to 35.2° and a

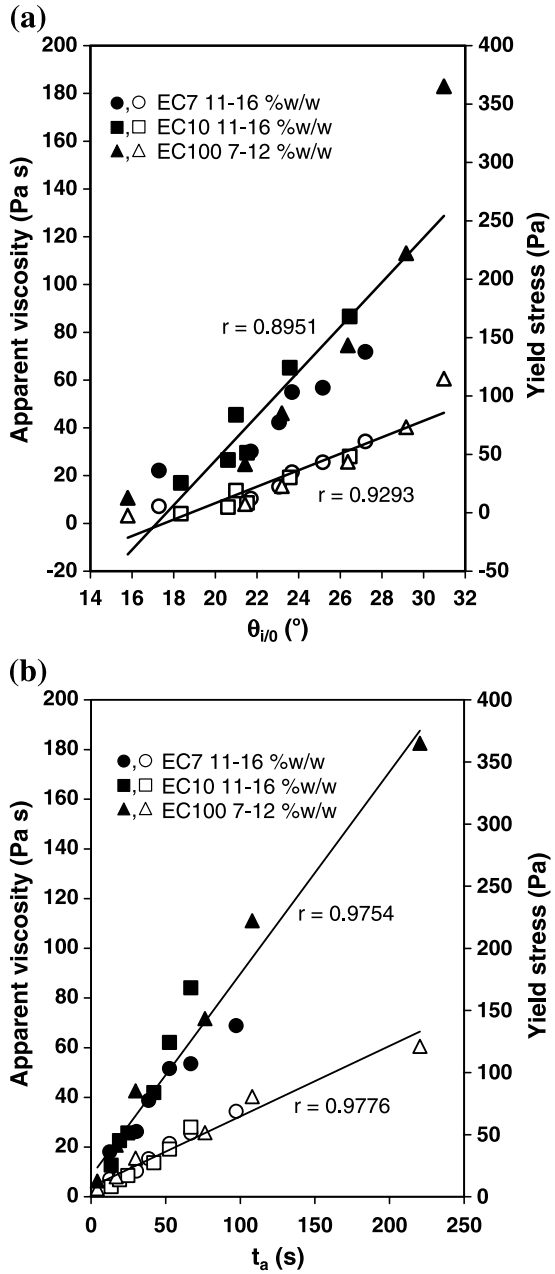

Fig. 7. Linear regressions of apparent viscosity and yield stress with (a) initial contact angle of sessile IPM drop, $\theta_{i/0}$, and (b) time for complete IPM absorption, t_a, for the entire concentration range of EC gels. Open symbols represent apparent viscosity and closed symbols represent yield stress.

mean $\theta_{i/h}$ of 30.1 ± 3.3°. Time taken for a complete absorption, which indicated the rate of IPM absorption, ranged from 2.3 to 35.2 s. Such a wide range in absorption time could be attributed to biological variables in different human skin such as skin thickness, hydration level, and hair density.

Density of EC Gel Matrices

Densities of EC7, EC10, and EC100 ranged from 0.935 to 0.981, 0.939 to 0.993, and 0.927 to 1.032 g mL^{-1}, respectively. Coefficients of variation ranged from 0.06 to 1.26% for all samples. The density of all the EC gels was lower than that of water (0.998 g mL^{-1}) at 22°C, except 12% w/w EC100, which was slightly denser (1.032 ± 0.003 g mL^{-1}). Gel densities increased linearly with concentration of EC7 (r = 0.9782) and EC10 (r = 0.9909), but increased exponentially for EC100 (Fig. 6).

Correlation of EC Gel Wetting Behavior with Rheological and Mechanical Properties

It was postulated that the rheological and mechanical properties of EC gels would affect their wetting behavior. Hence, an attempt was made to correlate the wetting parameters with the rheological and mechanical parameters of EC gels via linear regression. Oscillatory rheological parameters (elastic moduli), continuous rheological parameters (apparent viscosity at shear rate of 10 s^{-1}, yield stress, and area of hysteresis), and mechanical parameters (hardness and adhesiveness) were employed in the linear regression analysis (Table VI). These parameters were adopted from a previous study on EC gel rheology and mechanical properties (1). The contact angles (θ_w and θ_i) and standing volumes (V_w and V_i) generally exhibited satisfactory linear correlation with both rheological and mechanical parameters, with r values ranging from 0.7314 to 0.9956, respectively. Comparing between rheological and mechanical parameters, the former (mean r = 0.9318) showed a better correlation with wetting parameters than the latter (mean r = 0.9150). θ_i was better correlated with apparent viscosity and yield stress because the relationship could be described by a single regression line irrespective of the grade of EC (r = 0.9293 and 0.8951, respectively). Among the parameters that represented rate of wetting, t_a showed the most satisfactory linear correlation with r ranging from 0.9133 to 0.9979 (Fig. 7).

DISCUSSION

A liquid drop in contact with a surface will exhibit a contact angle at the three-phase contact line. Dynamic contact angle refers to contact angle formed at a moving liquid front (24). The dynamic contact angles measured for the sessile liquid drops in the current study were advancing contact angles formed when the liquid front advanced on the gel–air interface. By definition, complete wetting, partial wetting, and nonwetting conditions occurred when $\theta = 0°$, $0° < \theta < 90°$, and $\theta \geq 90°$, respectively (22). The nonaqueous EC gels studied were thus partially wetted by water and completely wetted by IPM.

Information about surface configuration and hydrophilic–lipophilic properties of EC gels could be obtained from the dynamic contact angle profiles of water and IPM on the gel surfaces. Water is commonly used as a liquid possessing good hydrophilic property. IPM consisting of isopropyl ester of myristic acid (C_{14}) is predominantly a lipophilic solvent. The ability of both water (hydrophilic) and IPM (lipophilic) to form sessile drops with contact angles of 44–61° and 16–31°, respectively, upon contact with EC gels proved that the gel matrices possessed both hydrophilic and lipophilic properties, with predominance of the latter. This observation agreed with the nonaqueous nature of the gel. IPM is usually employed to represent the polar/nonpolar nature of the skin (28). It has been used as a vehicle in partition coefficient experiments to predict the amount of drug partitioning into the skin (29). The good skin compatibility of IPM was demonstrated in the current study by the relatively low initial contact angle (≤35.2°) and short absorption time (≤35.2 s) of IPM drops placed on the skin of human subjects. The ready absorption of sessile IPM drops into EC gels and the overlap of the range of IPM contact angle values on EC gels (16–31°) with those on human skins (23–35°) implied a certain degree of similarity of the gel with the nature of the skin. This, in turn, would reflect good compatibility of the nonaqueous EC gel with human skin in its function as a topical gel.

EC is known to be a water-insoluble, hydrophobic polymer due to the hydrophobic ethyl substitution on its hydrophilic cellulose backbone. Entanglement of polymer chains and subsequent gelation of EC is brought about by intermolecular hydrogen bonding and dipole–dipole interaction involving the unethoxylated hydroxyl groups on the C-6 position of the anhydroglucose units of the EC backbone (1,30–33). The observed wetting behavior of EC gel matrices could be partially explained by change in the EC gel surface configuration upon contact with liquid sessile drops. The tendency of reorientation of polymeric moieties on gel surfaces to establish equilibrium with the surrounding medium in order to minimize interfacial free energy is well recognized. When the gel is exposed to air, a hydrophobic gel–air interface will exist where hydrophobic segments of the polymer and solvent chains are oriented toward the air phase, and hydrophilic moieties are buried in the interior of the gel matrix (11,15–17,34–36). The reasonably low θ_w observed for EC gels indicated the presence of hydrophilic moieties at the gel–water interface. This could be explained by reorientation by molecular rotation of flexible parts of the polymer and solvent to direct the unethoxylated and hydrophilic C_6 –OH groups directly beneath the drop toward the gel–water interface upon contact of EC gel surface with the sessile water drop. As surface mobility of functional groups was prevalent in polymeric materials at room temperature (36–39), such reorientation was highly possible in EC gel surfaces. This was even more favorable in semisolid gel as gel surface is highly perturbable (40). The time dependence of the dynamic contact angle could also be explained to some extent by this phenomenon, because time was needed for reorientation to occur before attaining equilibrium contact angle (37). Such reorientation was not necessary for gel wetting by IPM, as there would be favorable hydrophobic interaction with the hydrophobic EC gel–air interface.

Surface chemical heterogeneity due to the presence of microscopic patches of hydrophobic and hydrophilic groups

with differing surface energies as well as surface topography such as roughness had been reported to affect contact angle of sessile liquid drops on solid polymeric materials (36,39,41). The former could inhibit uniform wetting (37), whereas the latter might reduce the observed contact angle when $\theta < 90°$ (42). However, the significance of these factors was dependent on the polymeric system being studied. Roughness was not an important factor in well-prepared polymer surfaces as they were shown to be smooth (37,41), whereas polymer surfaces with different surface roughness and heterogeneity could demonstrate the same advancing contact angles (43). In general, surface roughness below 0.1–0.5 μm or heterogenous patch below 1 μm would induce negligible effect on the observed advancing contact angle (42,43). Although the influence of these factors on the contact angle of polymeric systems was acknowledged, their effect on EC gel wetting was not investigated in the current study. The influence of gel lipophilicity, rheological and mechanical properties on EC gel wetting behavior were the main focus of this study.

The observed dynamic contact angle of sessile liquid drop might be partly attributed to a slight solvation of gel materials, which affected the liquid drop surface tension and consequently the contact angle. However, the insolubility of EC and immiscibility of Miglyol 840 with water ensured negligible solvation effect. Greater solvation of the nonaqueous gel materials was expected for IPM because of their common lipophilic properties, hence resulting in lower sessile drop contact angle as compared to water. Given the enormous proportion of polymer and solvent relative to the sessile liquid drop, the same degree of solvation was expected to occur in each drop of liquid. Hence, solvation factor was deemed to be trivial in explaining the observed differences in trends of wetting of different EC gel formulations.

Polymeric chain length and concentration-dependent trends for the extent and rate of wetting were observed for all the EC gels studied. Higher EC concentration and greater polymeric chain length resulted in a lower extent of wetting by water as reflected by θ_w, V_w, $\theta_{w/e}/\theta_{w/0}$, and $V_{w/e}/V_{w/0}$ values. The effect of polymeric chain length was only apparent between EC with large difference in molecular weights such as between EC100 and EC7 or EC100 and EC10. Increased EC concentration and polymeric chain length gave rise to a higher degree of gel structuring to form a stiffer gel network due to the increased entanglement density associated with the number of intermolecular contacts per unit volume of EC gel (1). The resulting decrease in chain mobility would impose greater difficulty to rotational reorientation of C_6 –OH groups, hence reducing the number of –OH groups available to interact with the water sessile drop. This rendered a more lipophilic gel surface, which led to higher water contact angle.

IPM demonstrated similar trends as water where the extent and rate of gel wetting decreased with increased concentration and polymeric chain length although the more lipophilic EC gel matrices were expected to show greater affinity for lipophilic solvents such as IPM. In a study involving relatively solid substrates, it was found that contact angle was a function of surface properties, but relatively independent of bulk properties of the substrate (35). However, in another study, the dependence of contact angle on polymer gel bulk structures was observed (40). Hence, it was postulated that apart from hydrophilic–lipophilic properties, rheological and mechanical properties of EC gel matrices have an influence on their wetting behavior.

Rheological and mechanical characteristics exerted significant influence on the overall physical properties of EC gels (1). Such characteristics were important predictors of gel product performance, such as drug release kinetics (44,45) and bioadhesion (19,46). The direct positive linear correlation of θ_w, V_w, θ_i, and V_i with rheological and mechanical parameters verified the influence of these parameters on the wetting behavior of EC gel matrices. The absorption-dominated wetting of 7% w/w EC100 by water sessile drop could be attributed to the absence of a strong gel network structure due to insufficient polymer concentration for extensive intermolecular interactions (1).

Apart from polymeric chain length and concentration, the influence of polydispersity on rheology of colloidal dispersions had been well documented. Increase in polydispersity was reported to reduce elastic modulus, viscosity, yield stress, and shear-thinning properties by increasing the maximum packing fraction, which was defined as the concentration at which uniformly distributed particles touch each other (47–49). Similar trend was also observed in EC gel where values of rheological parameters decreased in the order of EC100 > EC10 > EC7 with the increase in EC polydispersity (1.7, 2.5, and 3.3, respectively). EC7 and EC10 were expected to possess higher maximum packing fraction where smaller polymer molecules could fit in the interstitial spaces of larger molecules, hence reducing their intermolecular interactions (47) and their resistance to flow due to the increase in free volume for the movement of smaller molecules (48). Thus, EC7 and EC10 produced less viscous gels that were more readily wetted by water and IPM as compared to EC100. Despite their difference in polydispersity, the wetting behavior between EC7 and EC10 was similar due to a small difference in M_w, hence demonstrating the stronger influence of the latter.

The polymeric network mesh size representing the average distance between consecutive physical entanglements provides a measure of porosity of the network (50–52). Gel with higher mesh size would occupy higher volume for a particular mass of gel and this would result in a lower gel density. Hence, gel density determined using EC gel samples in their swollen states was assumed to be inversely related to mesh size, and gel density values were employed as an indirect measure for EC gel mesh size in this study. A more structured gel network would possess lower mesh size due to more extensive polymeric chain entanglement to give a denser gel network. Decrease in mesh size with increase in EC concentration and polymeric chain length was reflected by higher gel density with higher EC concentration (Fig. 6). This, in turn, imparted greater resistance to liquid penetration into the gel matrices, thereby decreasing the extent of water and IPM absorption. This explained the better rheology–gel wetting correlation observed with IPM instead of water. Because wetting by IPM mainly involved absorption into the gel matrices, it was logical for the gel rheology to exert a more direct influence on the wetting process. The rate of water and IPM absorption as reflected by $t_{50\%}$ for V_w and t_a, respectively, also decreased due to the decrease in mesh size. The effect of EC gel mesh

size on the extent and rate of absorption of sessile liquid drops was more straightforward as this process involved direct movement of liquid into the gel matrices. As described above, EC gel wetting by IPM was essentially governed by absorption, hence the observed difference in wetting behavior of different EC gels could be explained by the mesh size factor. Because EC gel was shown to be highly compatible with IPM due to their lipophilic properties, gel lipophilicity thus became a secondary factor in influencing the wetting behavior of different EC gels by IPM. The exponential increase in t_a for EC100 mirrored the exponential trend of EC100 density (Figs. 5 and 6), hence highlighting the strong influence of mesh size on the rate of IPM absorption. As for EC gel wetting by water, increased mesh size would render spreading of sessile water drop more difficult due to the higher propensity of water absorption. The increased rate of water spreading of higher concentration range of EC100 gels as indicated by greater $K_{\theta w}$ and lower $t_{50\%}$ for A_w was attributed to low mesh size. Such drastic reduction in mesh size especially for 12% w/w EC100, as reflected by the exponential increase in EC gel density (Fig. 6), was able to induce slippage of the sessile water drop on the gel surface, thereby facilitating more rapid spreading despite the higher content of hydrophobic chain segments in 12% w/w EC100 gels. The lower density of 8–10% w/w EC100 gave rise to higher mesh size, hence lower rate of water spreading. The concentration-dependent increase in gel density at the lower concentration range of EC100 was probably not steep enough to result in a significant difference in the rate of water spreading among the gel samples. EC7 and EC10 gels exhibited an opposite trend of rate of water spreading with respect to EC concentration as reflected in the $t_{50\%}$ values for A_w (Fig. 4). Densities of EC7 and EC10 were much lower than that of 12% w/w EC100 even at a higher concentration range; consequently, the reduction in mesh size might not be sufficient to induce slippage on the gel surfaces. Although mesh size factor did not exert a significant effect on rate of water spreading in EC7 and EC10 gels, gel lipophilicity seemed to play a prominent role in this case, where higher polymer concentration resulted in lower rate of water spreading as the consequential increase in gel surface lipophilicity impeded the rapid movement of water front along the gel surface. Unlike IPM, water has lower compatibility with EC gels, hence lipophilicity of EC gel matrices became an important limiting factor in wetting by water. Mesh size and lipophilicity of the gel exerted opposing effects on the rate and extent of EC gel wetting by water, where the former increased but the latter decreased water spreading. The interplay of these two factors on the extent of water spreading gave rise to a stable base area ratio of 1.2 irrespective of the different formulations of EC gel.

Wetting of nonaqueous EC gel matrices could be divided into extent and rate of wetting, which were quantitatively represented by different parameters derived from dynamic contact angle measurement. Extent of wetting by hydrophilic liquid, such as water, which formed an equilibrium sessile drop on the gel matrices, could be represented by initial and equilibrium contact angle, standing volume, and base area. The initial/equilibrium ratio of these parameters was more reliable for comparison within the same type of EC gel. For lipophilic liquid that was completely absorbed into the EC gel matrices, such as IPM, extent of wetting was described by initial contact angle and standing volume. Base area that illustrated sessile drop spreading was not a meaningful parameter due to the absorption-dominated wetting of EC gel. The initial rate of wetting of EC gel by both water and IPM was represented by the first-order rate constants for contact angle, which were more reproducible than the rate constants for standing volume and base area. The $t_{50\%}$ values could be complementary in providing information on whether the observed trends of rate constants were governed by rate of spreading or absorption. Time taken for complete absorption was another useful parameter to describe the rate of IPM absorption into EC gel matrices. The average CV of the raw data for θ, A, and V of water and IPM were compared to determine the order of suitability of each parameter as a predictor of EC gel wetting. Both water and IPM exhibited similar trends: $CV_\theta < CV_A < CV_V$. The average CV of θ, A, and V for water was 3.3, 4.4, and 7.5%, respectively, which were about 3 times lower than the corresponding values for IPM. Hence, θ values were able to provide a more accurate assessment of the wetting behavior of the EC gel matrices, and higher reproducibility would be obtained when more hydrophilic liquid of lower absorption tendency was used.

The free energy change for a liquid to make contact and adhere to the subtrate, for a substrate to be completely immersed in the liquid, and for a liquid that is already in contact with the substrate to increase its area of contact is used to describe adhesional, immersional, and spreading wetting, respectively (26,27). Liquid absorption by EC gel was reflected by immersional wetting. The propensity for these three stages of wetting of EC gel by water was inversely related to EC polymeric chain length and concentration for a particular wetting liquid as evident from W_a, A_t, and S_c (Table III). Unlike water, IPM did not exhibit equilibrium wetting as observed from its complete absorption into EC gels; therefore W_a, A_t, and S_c between water and IPM were not directly comparable. Besides, for nonequilibrium wetting such as IPM, rate of wetting ($K_{\theta i}$ and t_a) was a more important determinant of the gel wetting behavior (26).

The mechanism responsible for both water and IPM absorption into EC gel matrices was likely to be molecular diffusion. The affinity of water molecules toward the nonaqueous EC gel was imparted by the unethoxylated and hydrophilic C_6–OH on EC backbone. The presence of a sessile water drop on EC gel surface would result in diffusion of water molecules into the gel matrix by interactions with C_6–OH via hydrogen bonding. However, the abundance of lipophilic groups that dominated the overall property of EC gel would impart resistance to the diffusion of water molecules, thus resulting only in limited water absorption. Unlike water, IPM possessed high affinity toward EC gel because of the lipophilic nature of both IPM and EC gel. Also, the miscibility of IPM with Miglyol greatly increased the ease for molecular diffusion of IPM into EC gel matrix to bring about a complete absorption.

Dynamic contact angle measurement established the lipophilic nature of the nonaqueous EC gel. The lipophilic EC gel surface would ensure minimal ambient moisture absorption, hence protecting moisture-sensitive drugs incorporated in the gel matrices from hydrolysis. In the presence of water, rapid change of EC gel surface configuration allowed wetting and

moderate water uptake into the gel matrices. Therefore, a certain degree of gel hydration was possible despite the nonaqueous nature of the gel formulations. The ability of the nonaqueous EC gel to be wetted and slightly hydrated upon contact with water is essential for bioadhesion (2–5) as well as drug release from the gel matrices (6–10). The latter is especially important for a water-soluble drug that is likely to exist as a suspension in EC gel. For such formulations, drug dissolution in the aqueous medium is required for its transport out from the gel matrices to the aqueous biological environment. The ease of wetting and IPM uptake into the gel matrices signified good compatibility of the EC gel matrices with skin, and this served as a prerequisite for bioadhesion.

CONCLUSIONS

This is the first study that demonstrated the feasibility of employing dynamic contact angle combined with axisymmetric drop shape analysis as a method to investigate the wetting behavior of nonaqueous gel matrices in their original semisolid forms. It has also explored an alternative method of examining water uptake ability of topical gels pertaining to bioadhesive capacity of the gel matrices on relatively "dry" substrates such as skin and buccal mucosa.

The initial and equilibrium contact angle, base area, and standing volume of sessile water drops, and the initial contact angle and standing volume of sessile IPM drops could be employed as predictors of the extent of EC gel wetting. The rate constant of the contact angle and time for complete absorption of liquid were suitable indicators of the rate of wetting.

The nonaqueous EC gel matrices possessed both hydrophilic and lipophilic properties as shown by their water and IPM wettability. The observed compatibility of the nonaqueous EC gel matrices with IPM in terms of wetting and absorption demonstrated their considerable lipophilic property and possibly good compatibility with skin because IPM exhibited satisfactory wetting with human skin. Increased EC concentration and polymeric chain length decreased the extent and rate of wetting as well as the thermodynamic driving force for the three stages of wetting, namely, adhesional, immersional, and spreading wetting. Although water and IPM absorption into EC gel matrices followed the same mechanism, namely, molecular diffusion, the ease and extent of molecular diffusion was hugely different because of the different nature of these liquids. The observed wetting behavior of EC gel was mainly governed by a balance between chemical and physical characteristics of the gel, namely, hydrophilic–lipophilic properties and rheological and mechanical properties, respectively. Rheological and mechanical properties were shown to play an influential role in dictating the gel surface configuration and mesh size of the gel network. The role of mesh size and hydrophilic–lipophilic factor was dependent on the type of penetrating liquid and EC gel formulation. The former factor played a more influential role in gel wetting by a lipophilic solvent and the latter generally served as a more important limiting factor for gel wetting by a hydrophilic solvent. The rate and extent of wetting could be modified by varying the EC/Miglyol ratio to give the desired gel wettability in view of the concentration-dependent wetting behavior of EC gels.

The ability of the nonaqueous EC gel matrices to adapt their surface configuration in response to the surrounding environment allowed them to serve as effective moisture barrier for moisture-sensitive drugs during storage and as easily wettable gel matrices upon application. The water and IPM wettability in turn serve as favorable properties for bioadhesion and drug release for topical drug delivery.

REFERENCES

1. P. W. S. Heng, L. W. Chan, and K. T. Chow. Development of novel non-aqueous ethylcellulose gel matrices: rheological and mechanical characterization. *Pharm. Res.* **22**(4):676–684 (2005).
2. N. A. Peppas and P. A. Buri. Surface, interfacial and molecular aspects of polymer bioadhesion on soft tissues. *J. Control. Release* **2**:257–275 (1985).
3. C. Lehr, J. A. Bouwstra, H. E. Boddé, and H. E. Junginger. A surface energy analysis of mucoadhesion: contact angle measurements on polycarbophil and pig intestinal mucosa in physiologically relevant fluids. *Pharm. Res.* **9**(1):70–75 (1992).
4. M. Toledano, R. Osorio, J. Perdigao, J. I. Rosales, J. Y. Thompson, and M. A. Cabrerizo-Vilchez. Effect of acid etching and collagen removal on dentin wettability and roughness. *J. Biomed. Mater. Res.* **47**(2):198–203 (1999).
5. P. Esposito, I. Colombo, and M. Lovrecich. Investigation of surface properties of some polymers by a thermodynamic and mechanical approach: possibility of predicting mucoadhesion and biocompatibility. *Biomaterials* **15**(3):177–182 (1994).
6. G. Buckton, M. Efentakis, H. Al-Hmoud, and Z. Rajan. The influence of surfactants on drug release from acrylic matrices. *Int. J. Pharm.* **74**:169–174 (1991).
7. G. Buckton. The role of compensation analysis in the study of wettability, solubility, disintegration and dissolution. *Int. J. Pharm.* **66**:175–182 (1990).
8. S. Spireas, S. Sadu, and R. Grover. *In vitro* release evaluation of hydrocortisone liquisolid tablets. *J. Pharm. Sci.* **87**(7):867–872 (1998).
9. R. Bodmeier and O. Paeratakul. Process and formulation variables affecting the drug release from chlorpheniramine maleate-loaded beads coated with commercial and self-prepared aqueous ethyl cellulose pseudolatexes. *Int. J. Pharm.* **70**:59–68 (1991).
10. V. Rosilio, M. L. Costa, and A. Baszkin. Wettability of drug loaded polymer matrices. *J. Dispers. Sci. Technol.* **19**(6–7): 821–841 (1998).
11. N. A. Peppas and N. K. Mongia. Ultrapure poly(vinyl alcohol) hydrogels with mucoadhesive drug delivery characteristics. *Eur. J. Pharm. Biopharm.* **43**:51–58 (1997).
12. C. Lehr, H. E. Boddé, J. A. Bouwstra, and H. E. Junginger. A surface energy analysis of mucoadhesion. II. Prediction of mucoadhesive performance by spreading coefficients. *Eur. J. Pharm. Sci.* **1**:19–30 (1993).
13. M. J. Rosa and M. N. Pinho. Membrane surface characterization by contact angle measurements using the immersed method. *J. Membr. Sci.* **131**:167–180 (1997).
14. E. Oh and P. E. Luner. Surface free energy of ethylcellulose films and the influence of plasticizers. *Int. J. Pharm.* **188**:203–219 (1999).
15. T. Yasuda and T. Okuno. Contact angle of water on polymer surfaces. *Langmuir* **10**:2435–2439 (1994).
16. K. Yamada, M. Minoda, T. Fukuda, and T. Miyamoto. Amphiphilic block and statistical copolymers with pendant glucose residues: controlled synthesis by living cationic polymerization and the effect of copolymer architecture on their properties. *J. Polym. Sci. Polym. Chem.* **39**:459–467 (2001).
17. W. Liu, B. Zhang, W. W. Lu, X. Li, D. Zhu, K. D. Yao, Q. Wang, C. Zhao, and C. Wang. A rapid temperature-responsive sol–gel reversible poly(*N*-isopropylacrylamide)-*g*-methylcellulose copolymer hydrogel. *Biomaterials* **25**:3005–3012 (2004).

18. P. E. Luner and E. Oh. Characterization of the surface free energy of cellulose ether films. *Colloids Surf. A* **181**:31–48 (2001).
19. I. G. Needleman, G. P. Martin, and F. C. Smales. Characterisation of bioadhesives for periodontal and oral mucosal drug delivery. *J. Clin. Periodontol.* **25**:74–82 (1998).
20. D. Y. Kwok, T. Gietzelt, K. Grundke, H. J. Jacobasch, and A. W. Neumann. Contact angle measurements and contact angle interpretation. 1. Contact angle measurements by axisymmetric drop shape analysis and a goniometer sessile drop technique. *Langmuir* **13**:2880–2894 (1997).
21. J. A. Dean. *Lange's Handbook of Chemistry*, 15th ed., McGraw-Hill, New York, 1999, p. 5.87.
22. G. Garnier, J. Wright, L. Godbout, and L. Yu. Wetting mechanism of alkyl ketene dimers on cellulose films. *Colloids Surf. A* **145**:153–165 (1998).
23. V. M. Starov, S. R. Kostvintsev, V. D. Sobolev, M. G. Velarde, and S. A. Zhdanov. Spreading of liquid drops over dry porous layers: complete wetting case. *J. Colloid Interface Sci* **252**:397–408 (2002).
24. S. Wu. Dynamic contact angles and wetting kinetics. *Polymer Interface and Adhesion*, Marcel Dekker, Inc., New York, 1982, pp. 235–255.
25. M. C. Wilkinson and T. A. Elliott. Dynamic contact angle in mercury/carbon tetrachloride/solution systems. III. The mechanism and kinetics of spreading. *J. Colloid Interface Sci.* **48**(2):225–241 (1974).
26. M. J. Rosen. *Surfactants and Interfacial Phenomena*, Wiley, New York, 1989, pp. 240–275.
27. G. D. Parfitt. Fundamental aspects of dispersion. In *Dispersion of Powders in Liquids*, Wiley, New York, 1981, pp. 1–50.
28. J. Jaiswal, R. Poduri, and R. Panchagnula. Transdermal delivery of naloxone: *Ex vivo* permeation studies. *Int. J. Pharm.* **179**:129–134 (1999).
29. R. Panchagnula. Transdermal drug delivery of tricyclic antidepressants: feasibility study. *STP Pharma Sci.* **6**(6):441–444 (1996).
30. H. Itagaki, M. Tokai, and T. Kondo. Physical gelation process for cellulose whose hydroxyl groups are regioselectively substituted by fluorescent groups. *Polymer* **38**(16):4201–4205 (1997).
31. Y. Sekiguchi, C. Sawatari, and T. Kondo. A gelation mechanism depending on hydrogen bond formation in regioselectively substituted *O*-methylcelluloses. *Carbohydr. Polym.* **53**:145–153 (2003).
32. T. Kondo and T. Miyamoto. The influence of intramolecular hydrogen bonds on handedness in ethylcellulose/CH_2Cl_2 liquid crystalline mesophases. *Polymer* **39**(5):1123–1127 (1998).
33. R. Rodriguez, C. Alvarez-Lorenzo, and A. Concheiro. Rheological evaluation of the interactions between cationic celluloses and Carbopol 947P in water. *Biomacromolecules* **2**:886–893 (2001).
34. M. X. Xu, W. G. Liu, J. Wang, W. Gao, and K. D. Yao. Surface rearrangement of vinyl acetate and acrylate terpolymer adhesives investigated by dynamic contact angles. *Polym. Int.* **44**:421–427 (1997).
35. A. H. Hogt, D. E. Gregonis, J. D. Andrade, S. W. Kim, J. Dankert, and J. Feijen. Wettability and ζ potentials of a series of methacrylate polymers and copolymers. *J. Colloid Interface Sci.* **106**(2):289–298 (1985).
36. D. Park, B. Keszler, V. Galiatsatos, and J. P. Kennedy. Amphiphilic networks. 9. Surface characterization. *Macromolecules* **28**(8):2595–2601 (1995).
37. O. N. Tretinnikov and Y. Ikada. Dynamic wetting and contact angle hysteresis of polymer surfaces studied with the modified Wilhelmy balance method. *Langmuir* **10**:1606–1614 (1994).
38. H. Tan, X. Xie, J. Li, Y. Zhong, and Q. Fu. Synthesis and surface mobility of segmented polyurethanes with fluorinated side chains attached to hard blocks. *Polymer* **45**:1495–1502 (2004).
39. G. S. Ferguson and J. M. Whitesides. Thermal reconstruction of the functionalized interface of polyethylene carboxylic acid and its derivatives. In M. E. Schrader and G. I. Loeb (eds.), *Modern Approaches to Wettability. Theory and Applications*, Plenum, New York, 1992, pp. 143–177.
40. A. Suzuki and Y. Kobiki. Static contact angle of sessile air bubbles on polymer gel surfaces in water. *Jpn. J. Appl. Phys.* **38**:2910–2916 (1999).
41. H. Rangwalla, A. D. Schwab, B. Yurdumakan, D. G. Yablon, M. S. Yeganeh, and A. Dhinojwala. Molecular structure of an alkyl-side-chain polymer–water interface: origins of contact angle hysteresis. *Langmuir* **20**:8625–8633 (2004).
42. S. Wu. Interfacial thermodynamics. *Polymer Interface and Adhesion*, Marcel Dekker, New York, 1982, pp. 1–28.
43. K. Grundke, D. Pospiech, W. Kollig, F. Simon, and A. Janke. Wetting of heterogenous surfaces of block copolymers containing fluorinated segments. *Colloid Polym. Sci.* **279**:727–735 (2001).
44. M. M. Talukdar, I. Vinckier, P. Moldenaers, and R. Kinget. Rheological characterization of xanthan gum and hydroxypropylmethylcellulose with respect to controlled-release drug delivery. *J. Pharm. Sci.* **85**(5):537–540 (1996).
45. D. S. Jones, A. D. Woolfson, J. Djokic, and W. A. Coulter. Development and mechanical characterization of bioadhesive semi-solid, polymeric systems containing tetracycline for the treatment of periodontal diseases. *Pharm. Res.* **13**(11):1734–1738 (1996).
46. S. Tamburic and D. Q. M. Craig. A comparison of different *in vitro* methods for measuring mucoadhesive performance. *Eur. J. Pharm. Biopharm.* **44**:159–167 (1997).
47. P. F. Luckham and M. A. Ukeje. Effect of particle size distribution on the rheology of dispersed systems. *J. Colloid Interface Sci.* **220**:347–356 (1999).
48. R. Greenwood, P. F. Luckham, and T. Gregory. The effect of diameter ratio and volume ratio on the viscosity of bimodal suspensions of polymer latices. *J. Colloid Interface Sci.* **191**:11–21 (1997).
49. D. M. Kalyon, E. Birinci, R. Yazici, B. Karuv, and S. Walsh. Electrical properties of composites as affected by the degree of mixedness of conductive filler in the polymer matrix. *Polym. Eng. Sci.* **42**(7):1609–1617 (2002).
50. A. M. Lowman and N. A. Peppas. Hydrogels. In E. Mathiowitz (ed.), *Encyclopedia of Controlled Drug Delivery*, Wiley, New York, 2000, pp. 397–417.
51. S. Baumgartner, J. Kristl, and N. A. Peppas. Network structure of cellulose ethers used in pharmaceutical applications during swelling and at equilibrium. *Pharm. Res.* **19**(8):1084–1090 (2002).
52. R. A. Gemeinhart and C. Guo. Fast swelling hydrogel systems. In N. Yui, R. J. Mrsny, and K. Park (eds.), *Reflexive Polymers and Hydrogels: Understanding and Designing Fast-Responsive Polymeric Systems*, CRC Press, Boca Raton, FL, 2004, pp. 245–257.